Close-Clearance Helical Impellers: A Physical Model for Newtonian Liquids at Low Reynolds Numbers

With simple hydrodynamic concepts, a physical model is developed to describe the flow at the wall close to the impeller blade. The parameters of this model were evaluated from the large amount of data on power consumption and checked with some independent data on velocity profiles. Together with the physical insight provided by the model, it helped to obtain general relationships for power and heat transfer coefficients. Equations for the latter were developed using Levêque's approximation. Agreement between the predicted results and the literature data of several independent studies was rather good. A method to analyze mixing or blending results is also suggested.

V. V. CHAVAN

Process Engineering Consultant
Bomendijk 19
3181 RE Rozenburg
The Netherlands

SCOPE

For many industrial operations, such as mixing or blending of liquids, dispersing pigments into liquids and heat transfer, and for polymerization, impellers like ribbons, screws or combined ribbon-screws were often used. These are proved to be particularly efficient with the highly viscous liquids and thus are often operated at low Reynolds numbers ($Re \leq 50$).

Research into the hydrodynamics in such vessels has began as early as 1956 and general flow patterns have been known since that time. Quantitative studies to a greater extent were undertaken in early 70's in a number of laboratories. Most available information is, however, on the power consumption. Some data on circulation capacities, mixing times and heat transfer have also been collected. Data have often been empirically correlated; although a couple of semitheoretical attempts were made, they neither provided the complete physical picture nor did they obtain general relationships. A model capable of putting the most of experimental data in a proper perspective, general enough to describe more than one phenomena like power consumption, mixing and heat transfer, and simple enough to be readily usable was therefore highly desired. Development and application of such a physical model is the subject of this paper.

CONCLUSIONS AND SIGNIFICANCE

Most of the literature data on velocity profiles, circulation capacities, power consumption, mixing times and heat transfer in vessels agitated by ribbons, screws in draft tube and combined ribbon have been thoroughly analyzed in this paper. The proposed hydrodynamic model has been successful in providing a basis to analyze transport phenomena in these agitated vessels.

Further, general relationships have been developed for predicting power consumption and heat transfer and are also useful for scale-up and extrapolation. The model also helps to quantitatively analyze the effect of geometrical variables such as the impeller pitch and the gap between the impeller and the vessel on the physical quantities. Several conclusions of such effects are elaborated. In summary, the proposed model and analysis provides a better understanding of the phenomena in these vessels which should help design better mixers and scale-up complex situations such as polymerization or fermentation reactors.

INTRODUCTION

Usefulness of close-clearance helical impellers, namely, ribbon, combined ribbon-screw and screws in a draft tube (Figure 1), has been proved (Hoogendoorn and den Hartog, 1969), and emphasized (Chavan and Mashelkar, 1980) previously. Several mixing equipment manufacturers have been making such equipments for food, pharmaceutical and polymer industries, where they are being used to perform such operations as blending of liquids, heat transfer or dispersion of solids into liquid. Often, they are used in reactors involving more than one of these operations. In recent years, therefore, a number of papers dealing with these impellers have appeared. Many of them report the measurements on power consumption (Nagata et al., 1970; Hall and Godfrey, 1970; Chavan and Ulbrecht, 1973b; Patterson et al., 1979) and some give data on mixing times (Coyle et al., 1970; Carreau et al., 1976; Kappel, 1979b) and circulation, especially axial, capacities (Chavan and Ulbrecht, 1973a; Carreau et al., 1976).

The experimental data of these studies were often empirically correlated. Some attempts (Bourne and Butler, 1969; Chavan and Ulbrecht, 1973b; Chavan et al., 1975a; Patterson et al., 1979) have been made to derive semitheoretical correlations. Although these may be considered to be better than the empirical ones, especially for extrapolation or scale-up, they have not been able to give a

V. V. Chavan is presently at the Mixing Equipment Mfg. Co., 21A, Jari-Mari Mandir Rd., Bandra (W), Bombay, India.
0001-1541-83-6733-0177-$2.00.

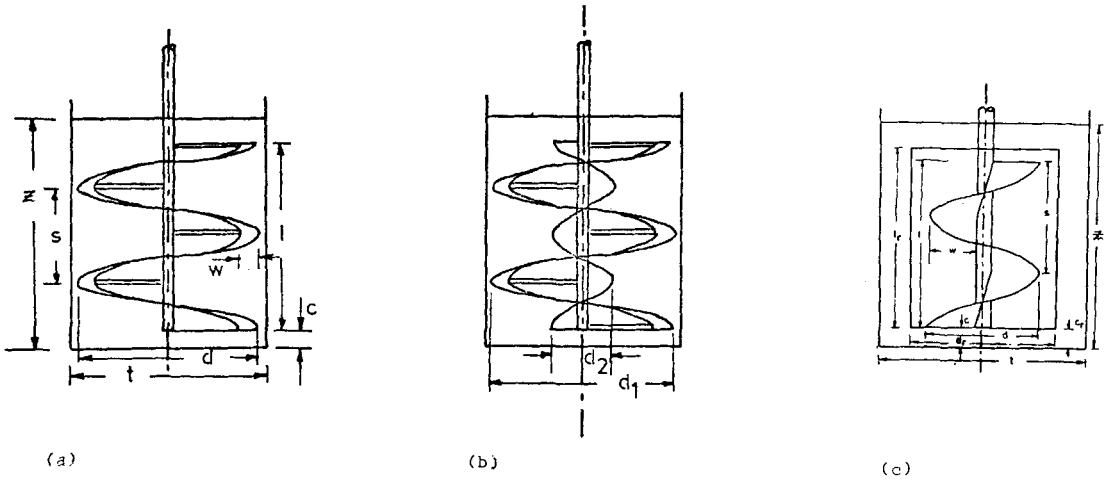

Figure 1. Close-clearance helical impellers: (a) ribbon impeller; (b) combined ribbon-screw impeller; and (c) screw impeller in a draft tube.

complete physical picture of the phenomena. This, in fact, is highly desirable to be able to quantify some of the items noted above.

General flow pattern in these geometries have been known for quite some time (Nagata et al., 1956). However, the quantitative studies on circulation capacities by Chavan and Ulbrecht (1973a) and Chavan et al. (1975a) and, especially, the detailed measurements on velocity profiles by Carreau et al. (1976) have revealed extremely useful information. Based on this, a physical picture of the hydrodynamics is derived. As a direct follow-up of this derivation, some of the operations noted above are analyzed quantitatively.

FLOW PATTERNS AND VELOCITY PROFILES

To simplify the further discussion, a brief description of the fluid motion will be useful. The primary motion of the impeller is tangential. As a direct result of this, rigid-body motion is created in the tangential direction; over and above this motion, there will be a displacement of liquid in the tangential and axial direction. As a ribbon impeller moves forward, for example, the liquid, pushed in the tangential direction (Figure 2), will flow backwards. The tangential velocity profile will then be created as a result of the rigid motion, the liquid displacement, and the fact that the velocity component at the wall is zero. The axial motion, in upward or downward direction, is created by the helical shape of the impeller. The liquid, pushed downwards by the impeller in the vicinity of the blade, will rise upwards through the center; thus completing the loop. The combined ribbon-screw impeller will essentially create similar flow, but axial flow may be intensified due to the presence of the screw. The axial-loop will be somewhat different for the screw in a draft tube, where the liquid, pushed downwards (or upwards) by the screw, will rise (or flow downwards) between the draft tube and the vessel.

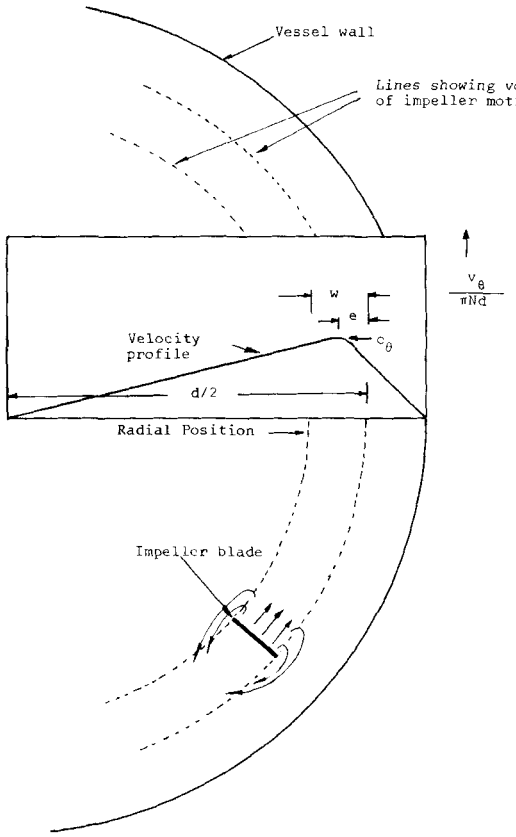

Figure 2. Velocity profile and flow patterns in a horizontal plane.

From the measurements of Carreau et al. (1976) with the ribbon impellers, it appears that the tangential velocity goes through a maximum value, which is about 0.44 times the tip speed for the Newtonian liquids. The maximum lies in the volume in which the impeller blade moves. The width of this volume is the same as that of the impeller (Figure 2). In the center, that is between the shaft and the blade, the liquid assumes a rigid body motion. The velocity profile is shown in Figure 2. Axial velocity has two maxima, one again lies in the impeller blade volume and the second one is at about one third of the vessel radius. The first one, which is of more relevance, does not show a sharp maximum and in fact it has the same value in the blade volume, which is about 0.08 of the tip velocity for the Newtonian liquids. It should be noted that these maximum values and their locations will depend, of course, on the impeller and the vessel geometries. The discussion that follows will consider these points in detail. Here it is sufficient to mention that the maximum values given above refer to the geometrical arrangement of Carreau et al. (1976).

Inside the draft tube with a rotating screw, tangential velocity is expected to be similar to that of a ribbon. Axial velocity profile will, however, be entirely different because the screw occupies the entire center region. The axial velocity, which is due to the pushing of the screw, is expected to increase with the radial position because of the increase in the total velocity along the impeller blade. On the other hand, zero velocity at the draft tube wall will have an inhibiting effect. Therefore, a flat velocity profile with a sharp drop near the draft tube wall is expected.

PHYSICAL MODEL

Figures 1 and 2 should be referred to for the geometrical variables, for the development of the physical model.

Velocity and Shear Rates

Dimensionless tangential and axial velocities are written as:

$$\bar{v}_\theta = \frac{v_\theta}{\pi N d} \tag{1}$$

$$\bar{v}_z = \frac{v_z}{\pi N d} \tag{2}$$

where d is the impeller diameter, and both $\bar{v}_\theta$ and $\bar{v}_z$ are functions of the radial position only. If c_θ and c_z are the maximum values of these dimensionless velocities, the shear rates at the vessel wall may be given by:

$$\dot{\gamma}_\theta = \frac{c_\theta \pi N}{\frac{1}{2}(\bar{t} - 1) + \bar{e}} \tag{3}$$

and

$$\dot{\gamma}_z = \frac{c_z \pi N}{\frac{1}{2}(\bar{t} - 1) + \bar{e}} \tag{4}$$

where t is the tank diameter, and e is defined as shown in Figure 2, $\bar{t}$ and $\bar{e}$ are (t/d) and (e/d). For a *screw with draft tube* of diameter, d_r, we will have:

$$\dot{\gamma}_\theta = \frac{c_\theta \pi N}{\frac{1}{2}(\bar{d}_r - 1) + \bar{e}} \tag{5}$$

and

$$\dot{\gamma}_z = \frac{c_z \pi N}{\frac{1}{2}(\bar{d}_r - 1) + \bar{e}} \tag{6}$$

where $\bar{d}_r$ is (d_r/d).

Force Balance

Tangential force F_θ at the tank wall will be the sum of the forces, due to the shear flow F_s which will be acting all along the tank wall and the one F_g acting on a thin belt opposite to the impeller, caused by converging-diverging flow near the gap. F_s is given by:

$$F_s = \mu(\dot{\gamma}_\theta)\pi t l \tag{7}$$

for the Newtonian liquids. F_g is rather difficult to define precisely because both the stresses and areas on which it acts are difficult to specify. F_g is then expressed as:

$$F_g = n_b f F_\theta \tag{8}$$

where n_b are the number of blades, and f defines F_g as the fraction of the total F_θ at the blade. Therefore:

$$F_\theta = \mu\dot{\gamma}_\theta \pi t l + n_b f F_\theta \tag{9}$$

for ribbon and combined ribbon screw. For screw impeller in a draft tube:

$$F_\theta = \mu\dot{\gamma}_\theta \pi d_r l_o + n_b f F_\theta \tag{10}$$

l_o is the length of the draft tube or the screw; whichever is smaller.

Power Consumption

Power consumption from the tangential force is:

$$P = F_\theta \pi t N \tag{11}$$

Using Eq. 9, power consumption becomes

$$P = \mu \left\{\frac{c_\theta}{1 - n_b f}\right\} \left[\frac{2\pi^3 t^2 l d N^2}{t - d + 2e}\right] \tag{12}$$

In the dimensionless form, the product of power number Po and Reynolds number Re is given by:

$$Po\,Re = \frac{P}{\mu d^3 N^2} = \left\{\frac{c_\theta}{1 - n_b f}\right\} \left[\frac{2\pi^3 \bar{t}^2 \bar{l}}{\bar{t} - 1 + 2\bar{e}}\right] \tag{13}$$

for the *ribbon or combined ribbon-screw impeller*. For a *screw impeller with a draft tube*, the equation is:

$$Po\,Re = \frac{P}{\mu d^3 N^2} = \left\{\frac{c_\theta}{1 - f}\right\} \left[\frac{2\pi^3 \bar{d}_r^2 \bar{l}_o}{\bar{d}_r - 1 + 2\bar{e}}\right] \tag{14}$$

Power may also be computed by summing up the power consumed by different mechanisms, for example, power for the shear flow near the wall P_s, power in the gap flow P_g and the power for pumping P_p. Thus:

$$P = P_s + P_g + P_p \tag{15}$$

P_p may be obtained if the pressure-drop Δp which causes the flow outside the region of direct impeller action is known together with the axial flow q. Chavan and Ulbrecht (1973a) have, for example, reported such measurements for the Newtonian liquids. Thus:

$$P_p = \Delta p q \tag{16}$$

Circulation Capacities

For ribbon and combined ribbon-screw impellers, the axial flow q is written as:

$$q = c_z \pi N d \pi d w n_b \tag{17}$$

The circulation number is:

$$Ci = \frac{q}{Nd^3} = c_z \pi^2 \bar{w} n_b \tag{18}$$

For screw in a draft tube, we have

$$q = c_z \pi N d \frac{\pi}{4} (d')^2 \tag{19}$$

where

$$d' = d - 2e \tag{20}$$

The circulation number becomes:

$$Ci = \frac{q}{Nd^3} = c_z \frac{\pi^2}{4} \bar{d}'^2 \tag{21}$$

Heat Transfer

With the knowledge of the velocity profiles, the derivation of heat transfer coefficients is somewhat straight-forward task. The maximum tangential velocity $(c_\theta \pi N d)$ is expected to be much larger than the maximum axial velocity $(c_z \pi N d)$. The latter appears to be smaller, by a factor of 6, than the former. For the convective heat transfer near the vessel wall, therefore, the influence of the axial velocity profile may be neglected. With this assumption, the heat transfer coefficient, based on the difference between the wall temperature and the well-mixed bulk liquid temperature, is obtained using the Lévêque's approximation (Pigford, 1955) as:

$$h = \frac{3^{1/3}}{2(\frac{1}{3})!} \left(\frac{k^2 c_p \rho \dot{\gamma}_\theta}{\pi t}\right)^{1/3} \tag{22}$$

for the *ribbon* (or *combined ribbon-screw*) impeller when the heat transfer is through the *jacketted vessel wall*. The equation is also written, after the substitution of $\dot{\gamma}_\theta$ from Eq. 3 as:

$$\frac{hd}{k} = 0.808 \left(\frac{c_\theta}{\bar{t}\{\frac{1}{2}(\bar{t} - 1) + \bar{e}\}}\right)^{1/3} \left(\frac{Nd^2 c_p \rho}{k}\right)^{1/3} \tag{23}$$

The draft tube is often a hollow cylinder through which a cooling or heating medium is passed. Sometimes it is made from helically wound tubes. In both of these cases, it is the heat transfering surface. For a *screw impeller* rotating inside such a draft tube, the heat transfer coefficient is given by:

$$\frac{hd}{k} = 0.808 \left(\frac{c_\theta}{\bar{d}_r\{\frac{1}{2}(\bar{d}_r - 1) + \bar{e}\}}\right)^{1/3} \left(\frac{Nd^2 c_p \rho}{k}\right)^{1/3} \tag{24}$$

EVALUATION OF PARAMETERS

In developing the physical model in the previous section, four physical parameters have been introduced. These are the dimen-

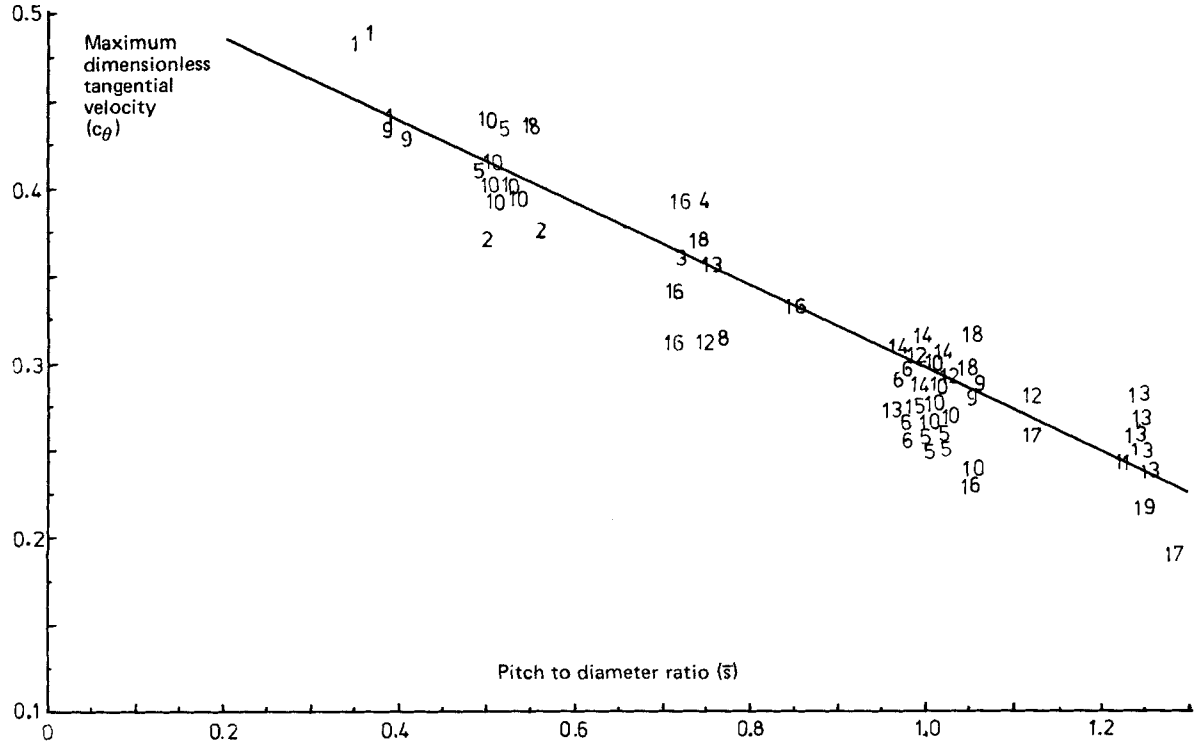

Figure 3. Maximum dimensionless tangential velocity c_θ for ribbon impeller: 1 = Bourne and Butler (1969); 2 = Edwards et al. (1981); 3 = Gluz and Pavluschenko (1966); 4 = Gray (1963); 5 = Hall and Godfrey (1970); 6 = Havas et al. (1978); 7 = Hoogendoorn and den Hartog (1969); 8 = Johnson (1967); 9 = Kappel and Seibring (1970); 10 = Kappel (1979b); 11 = Muller (1971); 12 = Nagata et al. (1956); 13 = Nagata et al. (1970); 14 = Nagata et al. (1972); 15 = Novak and Rieger (1969); 16 = Patterson et al. (1979); 17 = Reher and Boehm (1970); 18 = Takahashi et al. (1980); 19 = Ulrich and Schreiber (1967).

sionless maximum tangential velocity c_θ, the distance (e) between the radial point at which the maximum velocity occurs and the radial position of the impeller tip (Figure 2), and the factor f defining the fraction of total tangential force acting on a vertical belt opposite to the tip of the impeller, and the dimensionless maximum axial velocity c_z. These parameters may be evaluated from the detailed velocity measurements. These, however, are not always available. Data on power consumption are in such cases extremely useful.

Ribbon Impeller

Most relevant power data were those of Kappel (1979b). These data were collected in a systematic way where geometrical variables $\bar{t}$, $\bar{s}$ and n_b were varied. From such data, it was possible to compute both c_θ and f by solving the two algebraic equations obtained for $n_b = 1$ and $n_b = 2$. Assuming $\bar{e} = \bar{w}/2$, f always had a value of "0.3" and that c_θ did not depend on the ratio of tank to impeller diameter, but was very much dependent on the pitch to diameter ratio.

From the analysis of Kappel's data, it appears that f is independent of the geometry and has a value of 0.3. This is encouraging, because now it is possible to examine the rest of the literature data with this premise. Before any computations, however, we examined the literature data carefully, to get rid of any inconsistencies. For example, it was found that Zlokarnik (1967) gives about 50% higher values for $(P/\mu d^3N^2)$ compared to those of Kappel (1979b) for the geometrically similar equipment. Kappel's other data being very much in agreement with those of several other workers (Nagata et al., 1956; Patterson et al., 1979) it was decided to discard Zlokarnik's data from our analysis. For similar reasons, the data of Zlopt and Moser (1964) was not considered; their values $(P/\mu d^3N^2)$ being much lower than the other's for a similar geometry. For example, their $(P/\mu d^3N^2)$ was about 80% lower than of Nagata et al. (1970). For the rest of the reported studies on 71 geometrical setups, the maximum dimensionless tangential velocity c_θ was computed. Except for one geometrical setup of Nagata et al. (1970), where the tank to the impeller diameter had extraordinarily high value of 1.58, the data from the rest showed that there is a simple relationship between c_θ and the pitch to diameter ratio $\bar{s}$. The relationship is shown in Figure 3. Further, using linear regression analysis, a simple relation:

$$c_\theta = 0.532 - 0.238\,\bar{s} \tag{25}$$

was derived.

It should be noted that in obtaining the above equation, f was 0.3 and $\bar{e}$ was 0.05. It should be emphasized that these values will depend on the geometrical variables. For example, f is expected to vary with the gap between impeller and the tank wall, $(\bar{t} - 1)$, and $\bar{e}$ may change with the blade width $\bar{w}$. Such dependence is assumed to be negligible within the range of geometries studied.

The decrease in the maximum tangential velocity with the increase in the pitch to diameter ratio can be understood with the help of some qualitative arguments as follows. When the pitch to diameter ratio approaches zero, that is when a ring impeller is rotating in the vessel, the maximum tangential velocity will approach the maximum value of the tip velocity, $c_\theta = 1$. As the ratio deviates from zero, the liquid on this ring is no longer carried by the impeller, but it is occasionally (once in 1/N·s) pushed by the impeller. Between the two successive pushes, the velocity will slightly damp down and will also be adversely influenced by the liquid that is pushed backwards by the impeller as it moves forward. The fluid motion in this period, however, will be greatly assisted by the impeller blades above and below any fluid points. Figure 4 explains this concept more clearly. The impeller blades above and below a fluid point are expected to greatly determine its tangential velocity by the way of induced shear flow. For a given impeller diameter, as the pitch is increased, the impeller blades are displaced vertically away from a fluid point; thus, reducing its tangential motion. An extreme case will be the motion due to a paddle or when the pitch to diameter ratio approaches infinity. Here the tangential motion is only due to the successive pushes due to the impeller. One would expect, therefore, the maximum dimen-

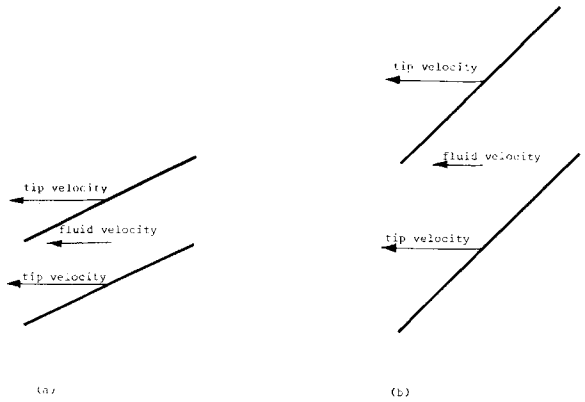

Figure 4. Influence of vertical position of impeller blades on tangential fluid velocity: (a) low pitch to diameter ratio; and (b) high pitch to diameter ratio

sionless tangential velocity c_θ to reach some asymptotic value as the pitch to diameter ratio $\bar{s}$ approaches infinity. The linear relationship (Eq. 25 and Figure 3) is, therefore, valid only in the limited range of $\bar{s}$; namely, $0.36 \leq \bar{s} \leq 1.25$.

In addition to the above mechanism, there is another explanation for the noted effect. The liquid that is pushed backwards by the motion of the impeller, the so-called leakage-flow, causes largely the deviations of the tangential velocity from the tip speed. The total liquid, pushed by the impeller, is divided into two parts, a part being pushed horizontally backwards and the rest vertically downwards (or upwards). The vertically downwards flow, the so-called axial flow, would to a certain extent (Appendix) depend on the pitch to diameter ratio. The higher the ratio, the lower the axial flow and therefore higher the leakage flow. Higher leakage flow means lower tangential velocities.

It should also be noted that the values of c_θ for two different geometries of Patterson et al. (1979), where $\bar{w}$ was varied by a factor of 2, differed only by 10%. This suggests that the assumption $2\bar{e} = 0.1$ is applicable in a wider range, namely, $0.1 \leq \bar{w} \leq 0.2$.

The best test of Eq. 25 and the analysis is the comparison of the derived physical parameters with some independent measurements. The velocity measurements of Carreau et al. (1976) are extremely useful for us in this respect. The maximum dimensionless tangential velocity calculated from Eq. 25, for their geometrical setup (pitch to diameter ratio of 0.7), was 0.37 (±8%) compared to the average measured value of 0.44. The agreement is excellent considering the scatter in the data, which was sometimes as high as ±20%.

The maximum dimensional axial velocity was calculated from the limited data on axial flow due to Coyle et al. (1970) and Carreau et al. (1976), using Eq. 18. The results are given in Table 1. The maximum dimensionless axial velocity appears to decrease slightly with the increase in the pitch to diameter ratio. This is expected because the axial drag flow created by the impeller is proportional to $(\bar{s}^2 + \pi^2)^{-0.5}$ (Appendix). A strong influence on c_z is noted in the reduction in its value due to the increase in the gap; that is, the increase in $\bar{t}$. This is clearly due to the increase in the leakage flow, the part of the flow caused by the pushing of the impeller. Further, it appears from the data of Coyle (1970) that the influence of the impeller length on the axial flow (thus on c_z) is not as strong as the drag flow equation (Appendix) suggests. In fact, it is almost nonexistent. Most likely reasons are the two adverse effects of the length

TABLE 1. MAXIMUM DIMENSIONLESS AXIAL VELOCITY IN VESSELS WITH RIBBON IMPELLERS

Data	$\bar{t}$	$\bar{s}$	No. of Geometries	Axial Velocity c_z
Coyle et al. (1970)	1.06	0.5	3	0.046 to 0.053
Carreau et al. (1976)	1.11	0.72	4	0.04 and 0.05
	1.11	1.05	1	0.04
	1.37	0.85	1	0.03

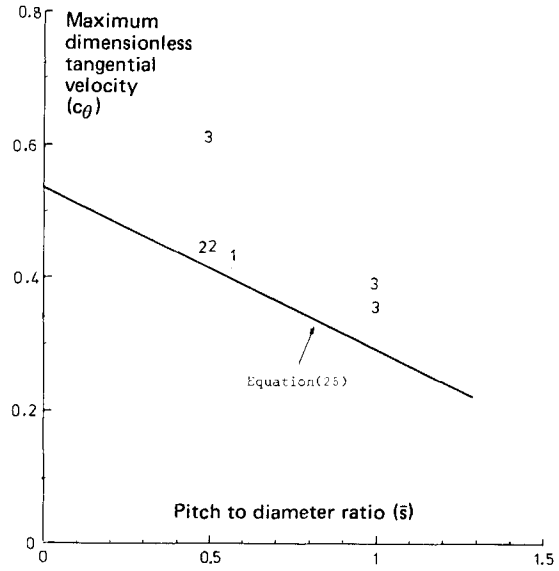

Figure 5. Maximum dimensionless tangential velocity for combined ribbon-screw impellers: 1 = Chavan and Ulbrecht (1973b); 2 = Havas et al. (1978); 3 = Nagata et al. (1972).

due to the frictional losses and gravity, which the flow will experience when completing the circulation loop.

Combined Ribbon-Screw Impeller

With the assumptions that:

$$f = 0.3 \text{ and } 2\bar{e} = 0.1,$$

the maximum tangential velocity was calculated using the ribbon equation (Eq. 13) for the nine geometrical arrangements for which data were available. The computed values of c_θ are shown in Figure 5. It appears that in most cases the ribbon equation (Eq. 25) is useful for the combined ribbon-screw impellers as well. It appears that when the screw is much smaller (the screw to ribbon diameter less than 0.33) than the ribbon, the influence of screw may be neglected.

Coyle et al. (1970) have shown that the circulation time is not greatly influenced by the presence of a screw, for the screw to ribbon diameter ratio being less than 0.33. It is, therefore, expected that c_z is also not greatly affected by the presence of an inner screw.

Screw Impeller in a Draft Tube

No detailed velocity measurements are available for this impeller, nor the possibility of directly exploiting the power data as was done for the ribbon. Further, the width to diameter ratio in this case is always ~0.4. This being much greater than that of a ribbon the assumption $2\bar{e} = 0.1$ is also unlikely to be reasonable. It was, therefore, decided to evaluate these parameters by curve fitting for a set of geometries.

Before using the data for any further analysis, it was critically assessed. It was found that the values of $(P/\mu d^3N^2)$ of Chavan et al. (1972) and Chavan and Ulbrecht (1973b) were always about 10 to 20% lower than the rest. The reasons have been elaborated by Chavan et al. (1975b). Most other workers have used torsion-bar dynamometers, which were calibrated under static conditions by using a pan and weight. Chavan et al. (1972) used a turntable, which was again statically calibrated. This gave torque values about 10% lower than what was dynamically (impeller rotating) calibrated. Dynamically calibrated torsion-bar dynamometer, on the other hand, gave 10 to 20% lower values than what would have been statically calibrated. The lower values of Chavan and Ulbrecht (1973b) are, therefore, due to their dynamic calibration. Without

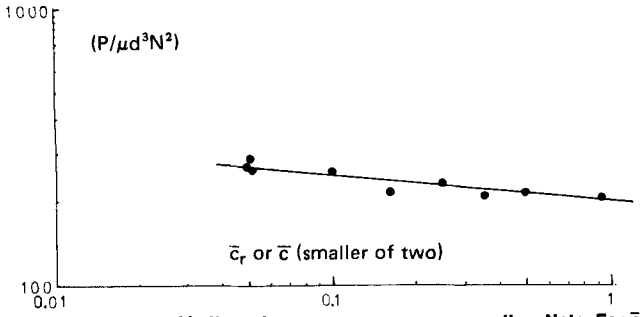

Figure 6. Influence of bottom clearance on power consumption: Note: For $\bar{s}$ = 1, $\bar{l}$ = 1.26 and $\bar{d}_r$ = 1.1; data of Nagata et al. (1957), Novak and Rieger (1977), and Sawinsky et al. (1979).

going into any further details, 20% was added to $(P/\mu d^3N^2)$ values of Chavan and Ulbrecht to bring them in line with the rest of the data.

One rather important difference between the screw in a draft tube and the ribbon is the flow at the bottom of the impeller. Systems with ribbon impellers are open and the liquid flow, when it is reversing the direction, is not obstructed as is in the screw system. The bottom clearance of the impeller or the draft tube whichever is lower will, therefore, have influence on the hydrodynamics inside the draft tube and on power consumption. The latter is well demonstrated in the Figure 6. To remove the complications brought in by this effect, we shall bring in a practical simplification. We shall consider only those data where the bottom clearance of screw or the draft tube is greater than 0.1, that is: $\bar{c}$ or $\bar{c}_r \geq 0.1$. Errors introduced by this simplication are ±10%.

Equation 14 may be written as:

$$\left(\frac{(P/\mu d^3N^2)\,(\bar{d}_r - 1)}{2\pi^3 \bar{d}_r^2 \bar{l}}\right) = -(2\bar{e})\left(\frac{P/\mu d^3N^2}{2\pi^3 \bar{d}_r^2 \bar{l}}\right) + \left(\frac{c_\theta}{1-f}\right) \quad (26)$$

If systematic data are available, it is, in principle, possible to evaluate $2\bar{e}$ and $(c_\theta/1-f)$ from this equation. Data should be from geometries, where $\bar{c}$ or $\bar{c}_r \geq 0.1$ and keeping $\bar{l}$ (and $\bar{l}_r$) and $\bar{s}$ constant and $\bar{d}_r$ the draft tube diameter is varied. From the available power data, six geometries did not qualify for the bottom clearance being very low and 11 geometries did not qualify for the second reason. The rate of the data gave straight lines between

$$\left(\frac{(P/\mu d^3N^2)\,(\bar{d}_r - 1)}{2\pi^3 \bar{d}_r^2 \bar{l}_o}\right) \text{ and } \left(\frac{(P/\mu d^3N^2)}{2\pi^3 d_r^2 \bar{l}_o}\right).$$

Plots between these two groups are shown in Figure 7. Calculated values of the parameters are summarized in Table 2.

It is interesting to note that for the screw impeller the maximum appears to be displaced inwards in comparison to the ribbon. Here, $2\bar{e}$ has a value between 0.12 and 0.15. Further, for the screw system being radially closed (blades extended up to the shaft), the maximum tangential velocity may also be expected to be higher than that in the ribbon system. f, the ratio representing the pressure drop at the impeller tip due to the flow in the gap between the screw and the draft tube wall may, however, have the same value as in the ribbon. Therefore, with the assumption that $f = 0.3$, c_θ was calculated and given also in Table 2. It is noteworthy that here also the maximum dimensionless tangential velocity decreased with the increase in the pitch. All the explanations given for the ribbon are also valid here.

The analysis of screw impeller data furnishes also a new information. The maximum tangential velocity decreases with the increase in the screw length. Since most of the data on ribbon impeller were for the geometries with $0.94 \leq \bar{l} \leq 1.20$, this aspect was not investigated for ribbon impellers. The decrease in the maximum tangential velocity may have been brought about because of the possible adverse effects (by the way of damping tangential motion) of the axial drag flow. Axial drag flow increases with the impeller length (Appendix). It is likely, therefore, that the maximum tangential velocity is reduced.

The circulation capacity data have been published by Chavan

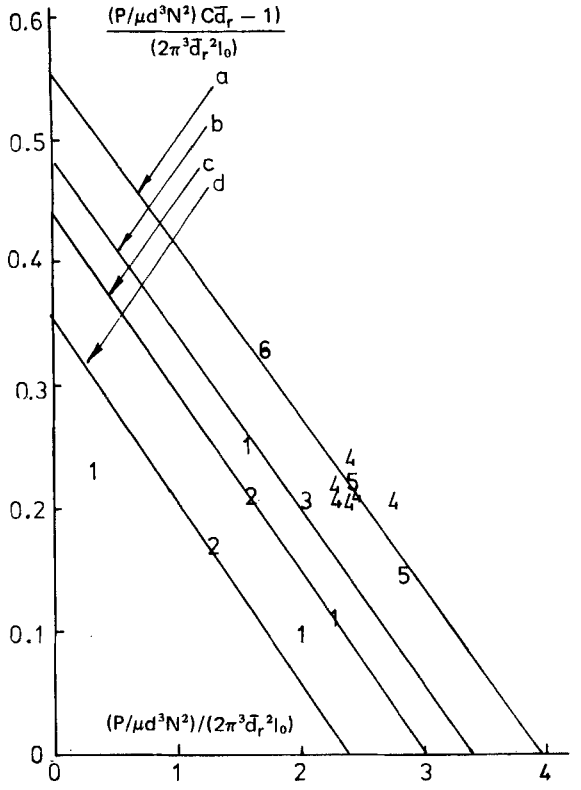

Figure 7. Power-data analysis for screw impellers with draft tube. Curves: a = ($\bar{s}$ = 1, $\bar{l}$ = 1.2 ± 0.05); b = ($\bar{s}$ = 1, $\bar{l}$ = 1.5 ± 0.05); c = ($\bar{s}$ = 1, $\bar{l}$ = 2.3 ± 0.05); d = ($\bar{s}$ = 0.5, $\bar{l}$ = 2.3 ± 0.05). Symbols: 1 = Chavan et al. (1972); 2 = Chavan and Ulbrecht (1973b); 3 = Nagata et al. (1957); 4 = Novak and Rieger (1977); 5 = Sawinsky et al. (1979); 6 = Seichter (1971).

and Ulbrecht (1973a). From part of these data $2\bar{e}$ was obtained (Table 2). For these c_z, the maximum dimensionless axial velocity (Eq. 21) was calculated for the screw impeller. The values again are given in Table 2.

As for the ribbon, the effect of the gap between the impeller and the nearby stationary wall is the strongest. Higher the pitch gap, thus also $\bar{d}_r$, the lower is the axial velocity. Origin of the pitch effect can again be found in the axial drag flow which suggests the effect as $(\bar{s}^2 + \pi^2)^{-0.5}$. The results in Table 2 also suggest the effect of the bottom clearance. Detailed discussion on this is already given by Chavan and Ulbrecht (1973a).

TABLE 2. PHYSICAL PARAMETERS FOR SCREW IN A DRAFT TUBE

(a) Maximum Tangential Velocities and Their Location

Pitch to Diameter $\bar{s}$	Smaller of $\bar{l}$ or $\bar{l}_r$	$2\bar{e}$	$(c_\theta/1-f)$	c_θ (If f Is Taken as 0.3)
0.5	2.3	0.14	0.43	0.3
1	2.3	0.12	0.31	0.22
1	1.2	0.15	0.56	0.39
1	1.5	0.15	0.48	0.34

(b) Maximum Axial Velocities in the Center Core of Diameter (d-2e)

$\bar{d}_r$	Smaller of $\bar{l}$ or $\bar{l}_r$	$\bar{s}$	Smaller of $\bar{c}$ or $\bar{c}_r$	Ci	c_z
1.16	1.5	0.96	0.104	0.055	0.115
1.05	2.25	0.5	0.156	0.159	0.337
1.05	2.25	1.0	0.156	0.212	0.46
1.74	2.25	1.0	0.156	0.22	0.047

$\bar{c}$ or $\bar{c}_r \geq 0.1$ and $1.05 \leq d_r \leq 1.2$ (one point in Figure 7 had $\bar{d}_r = 1.74$).

PRACTICAL IMPLICATION

A point, which especially arises in dealing with the axial flow impellers, needs some clarification, before any further discussion. Often, it has been stated (Chavan and Ulbrecht, 1973b; Mitsuishi and Miyairi, 1973) that the direction of flow, whether it is upwards or downwards near the impeller, has negligible influence on most of the integral or average physical quantities such as power consumption, circulation capacity, mixing times, or the heat transfer. All the equations and the discussions in the foregoing are, therefore, applicable for either direction of rotation.

Power Consumption

A summary of the physical parameters is given in Table 3 together with the range of their applicability. The range is determined on the basis of their suitability to predict the power consumption using Eqs. 13 and 14, which are the general relationships. It should be noted that the power thus calculated will be about 10–20% higher than the actual power consumed by the impeller, because of the typical calibration techniques used for the data in the literature.

Equation 15 shows the distribution of the total power P in three parts P_s, P_g and P_p. The last part, the power for pumping, was calculated for screws in a draft tube with the data of Chavan and Ulbrecht (1973a) and found it to be less than 3.5% of P. The ratio between P_g/P is expected to be equal to $n_b f$; thus, it is expected to be 0.3 or 0.6. It means, depending on the number of blades, the power for the gap flow is 30% (for one blade) or 60% (for two blades). The rest of the power is consumed for the shear flow at the vessel (or the draft tube) wall.

Shear Rates

Estimates of the shear rates at the walls of the vessel or the draft tube, both in the tangential and axial direction, are also possible using Eqs. 3 to 6. The accuracy of these equations is difficult to evaluate due to the lack of precise data. It may be noted, however, that the tangential shear rates have magnitudes of 10 to 25 s^{-1}; the values being close to those obtained by the wellknown Metzner-type analysis (Chavan and Mashelkar, 1980; Edwards et al., 1981).

TABLE 3. PHYSICAL PARAMETERS AND RANGE OF THEIR APPLICABILITY

(a) *Physical Parameters*

Physical Parameters	Ribbon Impeller*	Screw Impeller in a Draft Tube
Maximum Tangential Velocity, Dimensionless (c_θ)	0.532-0.238 $\bar{s}$	See Table 2
Displacement (Inwards) of the Maximum from the Impeller Tip, Dimensionless, ($\bar{e}$)	0.05	See Table 2
Tangential Force Due to the Gap-Flow at the Impeller Tip, As a Fraction of the Total (f)	0.3 per Blade	0.3
Maximum Axial Velocity, Dimensionless (c_z)	See Table 1	See Table 2

(b) *Range of Applicability*

Geometrical Variables	Ribbon[a]	Screw[b]
$\bar{t}$	1.02 to 1.37	1.5 to 3.96
$\bar{d}_r$ (for Screws Only)	—	1.08 to 1.74
Smaller of $\bar{l}$ or $\bar{l}_r$	0.94 to 1.20	1.15 to 2.35
$\bar{s}$	0.36 to 1.25	0.5 and 1
n_b	1 or 2	Always 1
$\bar{w}$	0.09 to 0.18	Always 0.4
Smaller of $\bar{c}$ or $\bar{c}_r$	Irrelevant	≥ 0.1
$\bar{z}$	1.05 to 1.8	1.5 to 3.96

* Also for combined Ribbon-screw for screw diameters smaller than one third of ribbon diameters.

[a] Errors ± 10% for "55" geometrical setups and ±25% when "71" are taken into account. $\bar{s} >$ 1.25 gives larger (i.e., ±25%) errors.

[b] Errors ± 10% except for one geometry when $\bar{d}_r$ was 1.74 (for which it was +25%).

Mixing and Blending Times

To assess the ability of an impeller to mix two liquids, the so-called mixing times θ_m are often measured (Coyle et al., 1970; Chavan et al., 1975a; Carreau et al., 1976; Ford and Ulbrecht, 1976). Kappel (1979a) has recently discussed this topic thoroughly showing that the precise values of the mixing time depend on many experimental factors; the important one being the end-point selection. Any generalizations derived from the data of several authors, therefore, can not be reliable. Our model may, however, lead to some useful relationships as follows. When the scale of scrutiny (Danckwerts, 1953; Chavan and Meshelkar, 1980), which is the scale at which a mixture is scrutinized, is much larger than the molecular scale and that the diffusion coefficients are extremely small, the laminar shear mixing approach (Chavan et al., 1975a; Walton et al., 1981) may be used to derive simple relations as follows. Let the thickness (the striation thickness) of a fluid element before and after the shearing in a given circulation loop be S_0 and S_1. The ratio S_1/S_0 will very much depend on the shear deformations (say $\dot{\gamma}_\theta N, \dot{\gamma}_\theta$ being much larger than $\dot{\gamma}_z$) and the elongational deformation [say $(\bar{t} - 1)^{-1}$ for ribbon] at the impeller tip. Simply,

$$\left(\frac{S_1}{S_0}\right) = B\left\{\dot{\gamma}_\theta N + \frac{n_b}{(\bar{t}-1)}\right\}^b \tag{27}$$

Equation 27 could be written for each circulation giving

$$\left(\frac{S_2}{S_1}\right), \left(\frac{S_3}{S_2}\right), \ldots\ldots\ldots\ldots$$

A product of all these gives

$$\frac{S_m}{S_0} = B_m\left\{\dot{\gamma}_\theta N + \frac{n_b}{(\bar{t}-1)}\right\}^{bm} \tag{28}$$

where m is the number of circulations required to complete the mixing that is to reach the required striation thickness S_m. The striation thickness, S_m, is the chosen scale of segregation (Danckwerts, 1953; Chavan and Mashelkar, 1980) which is the size of the clump of the unmixed component. S_m is much smaller than the scale of scrutiny. The number of circulations, m is also the ratio (θ_m/θ_c); θ_c being the circulation time. We have

$$\theta_c \propto \frac{z}{c_z \pi N d} \tag{29}$$

and

$$m \propto \frac{N\theta_m \pi c_z}{\bar{z}} \tag{30}$$

From Eqs. 28 and 30, we have

$$N\theta_m = \frac{M\bar{z}}{c_z \log\left\{\dot{\gamma}_\theta N + \frac{n_b}{(\bar{t}-1)}\right\}} \tag{31}$$

M is dependent on the segregation scale S_m and the initial volume of the liquid to be mixed, which is represented by S_0. M will, therefore, be dependent on the experimental techniques, especially the end-point selection. The other parameters $\dot{\gamma}_\theta$ and c_z may be calculated from Eqs. 3 and 18. For screw in a draft tube, the equation for $N\theta_m$ will be similar to Eq. 31 where $\bar{d}_r$ will appear instead of $\bar{t}$ and n_b will always be equal to 1. Equations 5 and 21 should then be used for $\dot{\gamma}_\theta$ and c_z.

On blending of two liquids of equal volumes (Chavan et al., 1975a; Ford and Ulbrecht, 1975) and on emulsification and dispersion of pigments at low Reynolds numbers data are rather scarce. Any physical analysis is only possible after considering such phenomena as the Rayleigh instabilities, the forces between par-

TABLE 4. PARAMETERS OF THE HEAT TRANSFER EQUATION FOR HELICAL RIBBON IMPELLERS

Reference	Geometry d	t	$\bar{s}$	n_b	Parameters of Eq. 32: Experimental α	x_1	x_2	x_3	Predicted by Our Model α	x_1	x_2
Edwards et al. (1981)	15	1.055	0.56	1	0.7	0.16	0.34	0.19	1.156	0.33	0.33
	40	1.068	0.5	1					1.146	0.33	0.33
Ishibashi et al. (1979)	14.8	1.047	1.04	2	2	0.33	0.33	0.14	1.1	0.33	0.33
	14.8	1.047	1.04	4							
Mitsuishi and Miyairi (1973)	38	1.053	1.0	2	0.78	0.33	0.33	0.14	1.05	0.33	0.33
Thomas (1972)	28.5	1.09	1	2	0.74				0.99	0.33	0.33
	29.9	1.04	1	2	1.0	0.33	0.33	0.18	1.07	0.33	0.33
	30.5	1.02	1	2	1.31				1.11	0.33	0.33

ticles or the strength of aggregates which are summarized by Chavan (1982).

Heat Transfer

Equations were derived earlier for the heat transfer coefficient to or from the walls closer to the impeller; namely, the vessel wall for the ribbon and the wall of the draft tube for a screw impeller. To compare these with the available data, we shall first write the heat transfer equation in a general form as:

$$Nu = \alpha(Re)^{x_1}(Pr)^{x_2}(Vi)^{-x_3} \tag{32}$$

where Nu (= hd/k), Re (= $d^2N\rho/\mu$), Pr (= $c_p\mu/k$), and Vi (= μ_w/μ) are various dimensionless numbers. When Eq. 32 is compared with Eqs. 23 and 24, x_1 and x_2 were found to be 0.33, which is a typical value at low Reynolds numbers. α is dependent on the geometry. x_3, of course, is not predicted by our equations and is always empirically determined. Parameters of Eq. 32, calculated from Eq. 23, are compared with those obtained from the data. The results of such comparison are shown in Table 4. With the exception of results of Edwards et al. (1981), the agreement is rather good. Figure 8, further, shows the comparison between Eq. 24 and the experimental data on screws in a draft tube. The agreement again appears to be excellent. Further, it should also be noted that the equations also correctly predict the dependence of the heat transfer on the geometry. It is found to increase with the decrease in the gap and to be independent of the number of impeller blades.

CONCLUSIONS

The model developed here not only provides physical insight into the hydrodynamics in the vessels agitated by ribbon and screw impellers, but also provides workable relationships to calculate power, shear rates, and heat transfer coefficients. This work suggested methods to analyze the mixing or blending in such vessels. The results of this work are useful only when the impeller Reynolds numbers are low ($\ll 300$). An exact limit is difficult to give because it is geometry-dependent. However, the results may safely be used for Reynolds number lower than 10 and, in general, they are applicable when the Power number Po is inversely proportional to the Reynolds number Re.

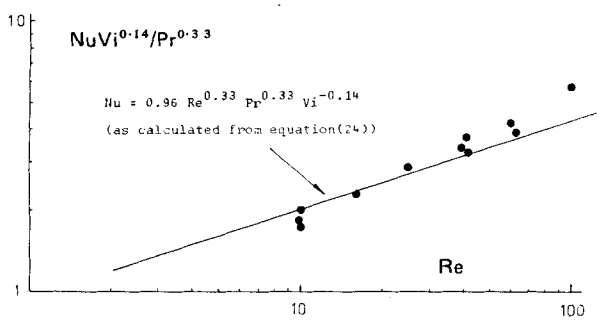

Figure 8. Heat transfer to a draft tube with a screw impeller in it. Note: For $\bar{d}$ = 0.21 m, $\bar{d}_r$ = 1.18, $\bar{s}$ = 1.06, $\bar{l}_r$ = 2.33, $\bar{l}$ = 2.79, $\bar{t}$ = 1.9, $\bar{z}$ = 3.1; data of Mitsuishi et al. (1973).

NOTATION

A = surface area of the impeller
b = exponent in Eq. 27
B = constant in Eq. 27
c = impeller clearance at the bottom
c_r = draft tube clearance at the bottom
c_p = specific heat
d = impeller diameter
d_r = draft tube diameter
e = distance between the point of the maximum tangential velocity and impeller tip
F = force
h = heat transfer coefficient
k = thermal conductivity
l = impeller length
l_o = l or l_r (smaller of two)
l_r = draft tube length
m = number of circulations
M = proportionality constant in Eq. 31
n_b = number of impeller blades
N = rotational speed
P = power consumption
Δp = pressure drop
q = axial discharge rate
s = pitch
S = striation thickness
t = tank diameter
v = velocity
w = width of impeller blade
x_1, x_2, x_3 = exponents in Eq. 32
z = liquid height

Subscripts

d = drag flow
g = gap flow
p = pumping
s = shear flow
z = axial direction
1,2 . . . . = for combined ribbon-screw impellers, "1" denotes ribbon and "2" screw; otherwise, they represent number of circulations
θ = tangential direction

Superscripts

$-$ = dimensionless variable (e.g., geometrical variables nondimensionalized with d are $\bar{t}$, $\bar{e}$ etc., and velocities nondimensionalized with πNd are $\bar{v}_\theta$, $\bar{v}_z$, etc.)

Greek Letters

α = constant in Eq. 32
$\dot{\gamma}$ = shear rate
θ_c = circulation time
θ_m = mixing time
μ = viscosity
ρ = density

Dimensionless Quantities

Ci = circulation number (q/Nd^3)
c_θ = maximum tangential velocity (maximum $v_\theta/\pi Nd$)
c_z = maximum axial velocity (maximum $v_z/\pi Nd$)
f = force at the impeller tip due to the converging-diverging flow in the gap as a fraction of total tangential force
Nu = Nusselt number (hd/k)
$N\theta_m$ = dimensionless mixing times
Po = Power number $(P/d^5N^3\rho)$
Pr = Prandtl number $(c_p\mu/k)$
Re = Reynolds numbers $(d^2N\rho/\mu)$

LITERATURE CITED

Bourne, J. R., and H. Butler, "Some characteristics of helical impellers in viscous liquids," *Trans. Inst. Chem. Engrs.*, **47**, T263 (1969).

Carreau, P. J., I. Patterson, and C. Y. Yap, "Mixing of viscoelastic liquids with helical ribbon agitators I—mixing time and flow patterns," *Can. J. Chem. Eng.*, **54**, 135 (1976).

Chavan, V. V., A. S. Jhaveri, and J. Ulbrecht, "Power consumption for mixing of inelastic non-Newtonian fluids by helical screw agitators," *Trans. Inst. Chem. Engrs.*, **50**, 147 (1972).

Chavan, V. V., and J. Ulbrecht, "Internal circulation in vessels agitated by screw impeller," *Chem. Eng. J.*, **6**, 213 (1973a).

Chavan, V. V., and J. Ulbrecht, "Dynamics of agitation of non-Newtonian liquids by close-clearance agitators," *Ind. Eng. Chem. Process Design Dev.*, **12**, 472 (1973b).

Chavan, V. V., D. E. Ford, and M. Arumagam, "Influence of fluid rheology on circulation, mixing and blending," *Can. J. Chem. Eng.*, **53**, 628 (1975a).

Chavan, V. V., P. J. Diggory, and J. Ulbrecht, "Influence of dynamometer calibration on the accuracy of the power consumption measurements," *Chemie Ing. Techn.*, **47**, No. 2, 74 (1975b).

Chavan, V. V., and R. A. Mashelkar, "Mixing of viscous Newtonian and non-Newtonian fluids," *Advances in Transport Processes*, A. S. Mujumdar, ed., Wiley Eastern, New Delhi (in U.S.A. and Canada, John Wiley & Sons, Inc., New York), **I**, 210 (1980).

Chavan, V. V., "Physical principles in suspension and emulsion processing," *Advances in Transport Processes*, A. S. Mujumdar, ed., Wiley Eastern, New Delhi (in U.S.A. and Canada, John Wiley & Sons, Inc., New York), **III** (1982).

Coyle, C. K., H. E. Hirschland, B. J. Michel, and J. Y. Oldshue, "Mixing in viscous liquids," *AIChE J.*, **16**, 903 (1970).

Danckwerts, P. V., "The Definition and Measurement of Some Characteristics of Mixtures," *Appl. Sci. Res.*, Sect A, **3**, 279 (1953).

Edwards, M. F., P. A. Shamlou, and H. Z. Wang, "Heat transfer in agitated vessels," *I. Chem. Eng. Symp. Ser.*, No. 64, The Institution of Chemical Engineers, London, England (1981).

Ford, D. E., and J. Ulbrecht, "Influence of rheological properties of polymer solutions upon mixing and circulation times," *Ind. Eng. Chem. Process Des. Dev.*, **15**, No. 2, T 321 (1976).

Ford, D. E., and J. Ulbrecht, "Blending of polymer solutions with different rheological properties," *AIChE J.*, **21**, No. 6, 1230 (1975).

Gluz, M. D., and I. S. Pawlushenko, "Power consumption in agitation of non-Newtonian liquids," *J. Appl. Chem.*, **40**, No. 7, 1430 (1967).

Gray, J. B., "Batch mixing of viscous liquids," *Chem. Eng. Prog.*, **59**, No. 3, 55 (1963).

Hall, K. R., and J. C. Godfrey, "Power consumption by helical ribbon impellers," *Trans. Inst. Chem. Engrs.*, **48**, T 20 (1970).

Havas, G., J. Sawinsky, and A. Deák, "Investigation of the homogenisation efficiency of the screw agitation, helical ribbon agitators, gate type anchor impeller and multi-paddle agitator in the mixing of high-viscosity Newtonian liquids," *Periodica Polytechnica. Chem. Eng.*, **22**, No. 4, 317 (1978).

Hoogendoorn, C. J., and A. P. den Hartog, "Model studies on mixers in viscous flow region," *Chem. Eng. Sci.*, **22**, 1689 (1967).

Ishibashi, K., A. Yamanaka, and N. Mitsuishi, "Heat transfer in agitated vessels with special types impellers," *J. Chem. Eng. Japan*, **12**, No. 3, 230 (1980).

Johnson, R. T., "Batch mixing of viscous liquids," **6**, 340 (1967).

Kappel, M., and H. Seibring, "Power requirements and mixing time in mixing time in the mixing of high viscosity liquids with helical impellers," *Verfahrenstechnik*, **4**, No. 10, 470 (1970).

Kappel, M., "Development and application of a method for measuring the mixture qualify of miscible liquids. I. State of research and theoretical principles," *Int. Chem. Eng.*, **19**, No. 2, 196 (1979a).

Kappel, M., "Development and application of a method for measuring the mixture quality of miscible liquids. III. Application of the new method for highly viscous Newtonian liquids," *Int. Chem. Eng.*, **19**, No. 4, 571 (1979b).

Mitsuishi, N., and Y. Miyairi, "Heat Transfer to non-Newtonian Fluids in an Agitated Vessel," *J. Chem. Eng. Japan*, **6**, No. 5 415 (1973).

Muller, W., "Auswahl and Auslegung von Ruhren zum Mischen zuher medien," *Dechema Monogr.*, **66**, No. 1193–1221, 247 (1971).

Nagata, S., M. Yanagimoto, and T. Yokoyama, "Studies of the power requirements of mixing impellers—III," Kyoto University, **18**, 444 (1956).

Nagata, S., T. Yanagimato, and T. Yokoyama, "A study of mixing of high-viscosity liquids," *J. Chem. Eng. Japan*, **21**, 278 (1957).

Nagata, S., M. Nishikawa, H. Tada, H. Hirabaryashi, and S. Gotoh, "Mixing of high viscosity liquids," *J. Chem. Eng. Japan*, **3**, 237 (1970).

Nagata, S., M. Nishikawa, T. Katsube, and K. Takaishi, "Mixing of highly viscous non-Newtonian liquids," *Int. Chem. Eng.*, **12**, No. 1, 175 (1972).

Novok, V., and F. Rieger, "Homogenisation with helical screw agitators," *Trans. Chem. Eng.*, **47**, 335 (1969).

Novak, V., and F. Rieger, "Influence of vessel to screw diameter ratio on efficiency of screw agitators," *Trans. I. Chem. Engrs.*, **55**, 202 (1977).

Patterson, W. I., P. J. Carreau, and C. Y. Yap, "Mixing with helical ribbons," *AIChE J.*, **25**, No. 3, 508 (1979).

Pigford, R. L., "Non-isothermal and heat transfer inside vertical tubes," *Chem. Eng. Prog. Symp. Ser.*, No. 17, **51**, 79 (1955).

Reher, E., and R. Boehm, "Ruehren Nicht-Newtonscher Fluessigkeiten," *Chem. Technik*, No. 3, 136 (1970).

Sawinsky, J., A. Deák, and G. Havas, "Power consumption of screw agitators in Newtonian liquids of high viscosity," *Chem. Eng. Sci.*, **34**, 1160 (1979).

Seichter, P., "Efficiency of the screw mixers with a draught tube," *Trans. Inst. Chem. Engrs.*, **49**, 117 (1971).

Takahashi, K., K. Arai, and S. Saito, "Power correlution for anchor and helical ribbon impellers in highly viscous liquids," *J. Chem. Eng. Japan*, **13**, No. 2, 147 (1980).

Thomas, R. R., "Heat transfer to high viscosity liquids in a helical ribbon impeller," PhD Thesis, University of Virginia (1972).

Ulrich, H., and H. Schreiber, "Stirring in viscous liquids," *Chemie Ing. Tech.*, **39**, 218 (1967).

Walton, A. C., S. J. Maskell, and M. A. Patrick, "Laminar mixing of non-Newtonian fluids in cylindrical vessels," *I. Chem. E. Symp. Ser.*, No. 64, The Institution of Chemical Engineers (1981).

Zlokarnik, M., "Suitability of stirrers for the homogenisation of liquid mixers," *Chem. Ing. Tech.*, **39**, 539 (1967).

Zopt, A., and F. Moser, "Auswahl eines Ruhrers fur die Emulsionpolymerization," *Verfahrenstechnik*, **8**, No. 1, 1 (1964).

Manuscript received December 9, 1981; revision received April 21, and accepted April 30, 1982.

APPENDIX: AXIAL DRAG FLOW

The axial drag flow q_d is given by:

$$q_d = \begin{pmatrix}\text{Downwards velocity}\\ \text{along impeller blade}\end{pmatrix} \times \begin{pmatrix}\text{Projected horizontal}\\ \text{impeller area}\end{pmatrix} \quad \text{(A.1)}$$

Supplementary material has been deposited as Document No. 04080 with the National Auxiliary Publications Service (NAPS), c/o Microfiche Publications, 214–13 Jamaica Ave., Queens Village, N.Y. 11428, and may be obtained for $4.00 for microfiche or $7.75 for photocopies.

$$= \pi dN \, \mathrm{Cos}\psi \qquad A \, \mathrm{Sin}\psi \, n_b \tag{A.2}$$

where ψ is the angle of the helix with the horizontal and A is its area. We have:

$$A/d^2 = \frac{\bar{l}\bar{w}\sqrt{\bar{s}^2 + \pi^2}}{\bar{s}} \tag{A.3}$$

and

$$\mathrm{Cos}\psi = \frac{\pi}{\sqrt{\bar{s}^2 + \pi^2}} \tag{A.4}$$

$$\mathrm{Sin}\psi = \frac{\bar{s}}{\sqrt{\bar{s}^2 + \pi^2}} \tag{A.5}$$

Axial drag flow is therefore:

$$q_d = \frac{\pi^2 d^3 N \bar{l}\bar{w} n_b}{\sqrt{\bar{s}^2 + \pi^2}} \tag{A.6}$$

Multivariable Control of a Wet-Grinding Circuit

The dynamic behavior of a pilot-plant grinding circuit was modelled by relating three output variables that were representative of the conditions within the mill and the classifier to three input variables, namely feed rates of the solids, mill water, and sump water.

A multivariable controller was designed, by the use of Inverse Nyquist Array techniques, for feedback control of the outputs by the inputs, and applied to the plant by a process-control computer with the use of direct digital control.

D. G. HULBERT

Council for Mineral Technology
Randburg, Republic of South Africa
and

E. T. WOODBURN

Department of Chemical Engineering
UMIST
Manchester, England

SCOPE

Grinding circuits contribute significantly to the capital and operating costs of mineral-processing plants, and much effort has therefore been expended on the understanding of these circuits and optimization of their design and operation. This paper describes a method used in the development of a multivariable control system for a grinding circuit and how the method was successfully applied to a pilot plant.

The control of a grinding circuit to an "operating point" can be regarded as the control of a number of important output variables (such as circulating load, conditions of classifications, and size of product) by means of plant input variables (such as the feed rates of solids and water). This poses a multivariable control problem that can be formulated as: identification of the relation between particular inputs and outputs and the design of a controller to control the outputs by maniputation of the inputs. The theory of linear dynamic systems is very useful in this application, and it is common practice for feedback control to be used to yield good responses that are insensitive to inaccuracies in the linear model of the plant.

Many attempts have been made to partition the multivariable control system by the selection of input-output pairs and the design of a controller for each pair (Gault *et al.*, 1979), since this enables the application of commercially available single-loop controllers. If the system is highly interactive (in the sense that each input has an appreciable effect on many of the outputs), the restricted structure of such a control scheme could result in poor control due to the interactions between the control loops. In practice, this would often result in one or more of the control loops not being implemented. However, the rapid development of digital hardware has made it economically feasible for a more sophisticated controller to be used that can implement full multivariable control. In general, such a controller computes changes in a number of inputs for each deviation of an output from its setpoint and has special provisions for dealing with interactions.

Inverse Nyquist array (*INA*) techniques were used for the design of a multivariable controller. The plant and the controller were considered in terms of their transfer-function matrices, and the *INA* provided a graphical means for the study of the stability of the system and its other characteristics. Fundamental theory relating to the *INA* can be found in a publication by Rosenbrock (1974), but some novel computational methods were used in this work for the derivation of a dynamic multivariable compensator.

CONCLUSIONS AND SIGNIFICANCE

A pilot grinding circuit has been successfully controlled by a dynamic multivariable controller in a way that allows stable operation at significant setpoints chosen by an operator. It is possible for three important variables relating to conditions within the mill and the classifier to be controlled.

The dynamic behavior of the plant was found to be highly interactive, but the use of INA techniques enabled a controller

Correspondence concerning this paper should be addressed to D. G. Hulbert.
0001-1541-83-6706-0186-$2.00.